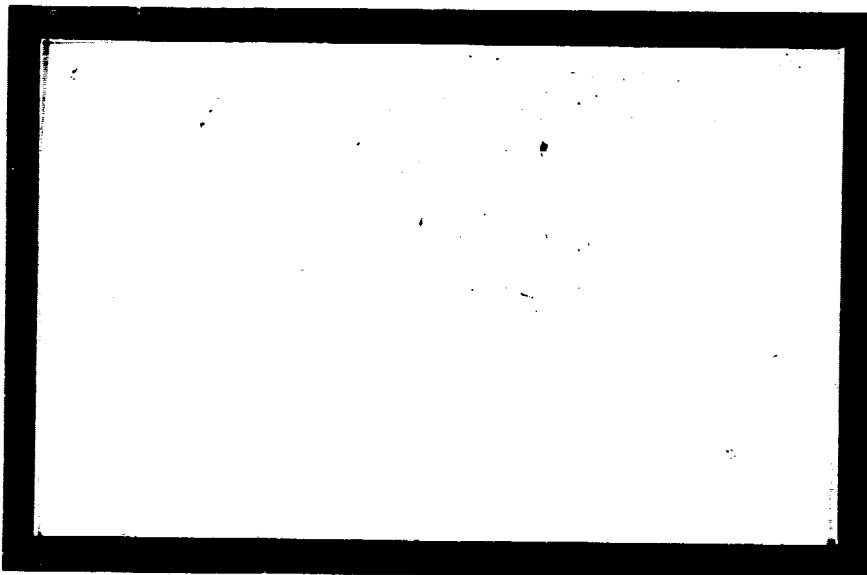


## **General Disclaimer**

### **One or more of the Following Statements may affect this Document**

- This document has been reproduced from the best copy furnished by the organizational source. It is being released in the interest of making available as much information as possible.
- This document may contain data, which exceeds the sheet parameters. It was furnished in this condition by the organizational source and is the best copy available.
- This document may contain tone-on-tone or color graphs, charts and/or pictures, which have been reproduced in black and white.
- This document is paginated as submitted by the original source.
- Portions of this document are not fully legible due to the historical nature of some of the material. However, it is the best reproduction available from the original submission.



(NASA-CR-170316) MATERIALS FOR  
HIGH-TEMPERATURE THERMOELECTRIC CONVERSION  
Annual Technical Report (Stanford Univ.)  
25 p HC A02/MP A01

N83-25035

CSCI 10A

Unclas  
G3/44 C3593



**CENTER FOR MATERIALS RESEARCH**

STANFORD UNIVERSITY • STANFORD, CALIFORNIA

Center for Materials Research  
McCullough Building  
Stanford University  
Stanford, CA 94305

9  
Y

Annual Technical Report  
on  
MATERIALS FOR HIGH-TEMPERATURE  
THERMOELECTRIC CONVERSION  
NASA Grant #NAGW-268  
Submitted to  
National Aeronautics and Space Administration  
CMR-83-2  
April 1983

Submitted by  
The Board of Trustees of  
Leland Stanford Jr. University  
Stanford, California 94305

Principal Investigator:  
Professor R. S. Feigelson  
Center for Materials Research  
Associate Investigator:  
Dr. D. Elwell  
Center for Materials Research

## ABSTRACT

This program has the main aim of developing materials of high efficiency for thermoelectric power generation, and capable of prolonged operation at temperatures over 1200°C. The present phase of the investigation has been focussed on high-boron materials.

Background theoretical studies have indicated that the low carrier mobility of materials with  $\beta$ -boron and related structures is probably associated with the high density of traps. These traps appear to be caused by physical defects rather than impurities, and it is planned to investigate their nature using high resolution electron microscopy.

Experimental work has been mainly concerned with silicon borides in view of promising data from European laboratories. A systematic study using structure determination and lattice constant measurements failed to confirm the existence of an "SiB<sub>n</sub>" phase. We found only SiB<sub>5</sub> and a solid solution of silicon in  $\beta$ -boron with a maximum solid solubility of 5.5-6 at % at 1650°C.

Hot pressing at GA Technologies gave encouraging samples of silicon borides and B<sub>6</sub>O. Our own hot press has now been delivered and will allow a rapid acceleration of our program. It is our conclusion that the material finally selected as the p-type leg of the thermoelectric generator will be a ternary composition with alloying elements chosen to optimize the carrier mobility and thermal conductivity.

TABLE OF CONTENTS

	<u>Page</u>
I. INTRODUCTION . . . . .	1
II. PREDICTIVE METHODOLOGY . . . . .	1
<u>Electrical</u>	
A. Conduction in $\beta$ -boron . . . . .	1
B. Solid solutions based on the $\beta$ -boron structure . . .	4
C. Thermal conductivity . . . . .	8
III. EXPERIMENTAL . . . . .	9
A. Silicon borides . . . . .	9
1. Phase diagram . . . . .	9
2. Crystal growth . . . . .	11
3. Solution growth . . . . .	12
4. Hot pressing . . . . .	13
B. Boron suboxide . . . . .	14
C. Thermal capacity of boron carbides . . . . .	15
D. Fiber crystal growth . . . . .	16
IV. SUMMARY OF MAIN CONCLUSIONS . . . . .	16
V. WORK PLAN . . . . .	17
VI. REFERENCES . . . . .	19

## I. INTRODUCTION

The main aim of this investigation is to develop materials for the next generation of thermoelectric energy conversion devices. In order to achieve a higher efficiency than that possible with generators utilizing silicon/germanium alloys, the new materials selected must be capable of long-term operation at a hot junction temperature of at least 1200°C. In addition to stability in vacuum, the essential requirement for the materials is a high thermoelectric figure-of-merit, defined by the parameter  $Z = \alpha^2 \sigma / K$ , where  $\alpha$  is the Seebeck coefficient,  $\sigma$  the electrical conductivity and  $K$  the thermal conductivity.

The development of p-type and n-type materials to meet the challenging requirement of  $ZT \approx 1$  over a temperature range from 600-1200°C will require a coordinated program of research and technology. The Stanford contribution is particularly aimed at an improved understanding of the most promising materials so that fundamental limitations can be identified, and efforts concentrated on key areas. The program therefore involves a study of the theory of the relevant material properties, the selection of materials which appear particularly promising, the fabrication of samples in polycrystalline and single crystal form, and the measurement and interpretation of their properties. Characterization studies in support of investigations at GA Technologies are also included, together with studies aimed at identifying totally new materials for this application.

This report describes the work performed during the second six-month period of the contract, from August 1982 until February 1983. During this period a second graduate student, Susumu Kusumoto, has joined this program, so that 5 people are now involved in the experimental investigations (K. N. Swamy Rao, Postdoctoral Research Associate, and Arie Ariotedjo, Research Assistant in addition to the investigators named on the title page). In addition, Professor B. Auld is spending 10% of his time working on theoretical aspects of the program.

## II. PREDICTIVE METHODOLOGY

### Electrical

#### A. Conduction in $\beta$ -boron

The general aim of this part of our program is to identify the factors that will permit the prediction of optimized high temperature thermoelectric

materials. Initially our study has been concentrated on high boron materials, since these appear the most promising of the known classes of candidate materials.

High-boron materials prepared from the melt or by a high temperature reaction normally exhibit the  $\beta$ -boron structure.  $\beta$ -boron has a rhombohedral structure with 105 atoms per unit cell (1) and with cell constants of  $a = 10.145 \pm .015\text{\AA}$  and  $\alpha = 65^\circ 17 \pm 8$ . The fundamental building block of high-boron materials is an icosahedron containing 12 boron atoms each bonded to five neighbors within the icosahedron. Since boron is trivalent, a structure in which each atom forms covalent bonds with 5 neighbors would be expected to be stable since each atom would then effectively have a full set of 8 electrons. However this simple situation is not the case in practice since each atom in the icosahedron is bonded to another atom outside its icosahedron. These extra bonds are directed radially outwards from the center of the icosahedron. Most atoms therefore have six-fold coordination, with an average bond length of  $1.75\text{\AA}$ . However, within the unit cell of 105 atoms, there are also 12 atoms of coordination number 8 and 2 with coordination number 9(1). These complexities make it very difficult to calculate the electron energy band structure with a reasonable degree of reliability.

$\beta$ -boron is a p-type semiconductor with a thermal band gap of 1.27 to 1.35 eV and an optical bandgap of 1.41-1.44 eV (2). The resistivity of purified material is normally in the range of  $10^5$ - $10^6$  ohm cm at room temperature and  $\approx 1$  ohm cm at 1000 K (see Fig 1) although Eubank et al. (3) observed a resistivity two orders higher over a wide temperature range in a needle-shaped single crystal of material purified by vaporization at  $\approx 2050^\circ\text{C}$ . The slope of the graphs shown in Fig 1 is around 0.7 eV, which suggests intrinsic conductivity if the band gap is  $\approx 1.4$  eV as suggested by the review of data quoted above (2). The observation of p-type behavior of the Seebeck coefficient is therefore presumed to be associated with a relatively large hole mobility compared with the electron mobility. Since the hole mobility is low, the conduction electrons must be strongly trapped.

ORIGINAL PAGE IS  
OF POOR QUALITY

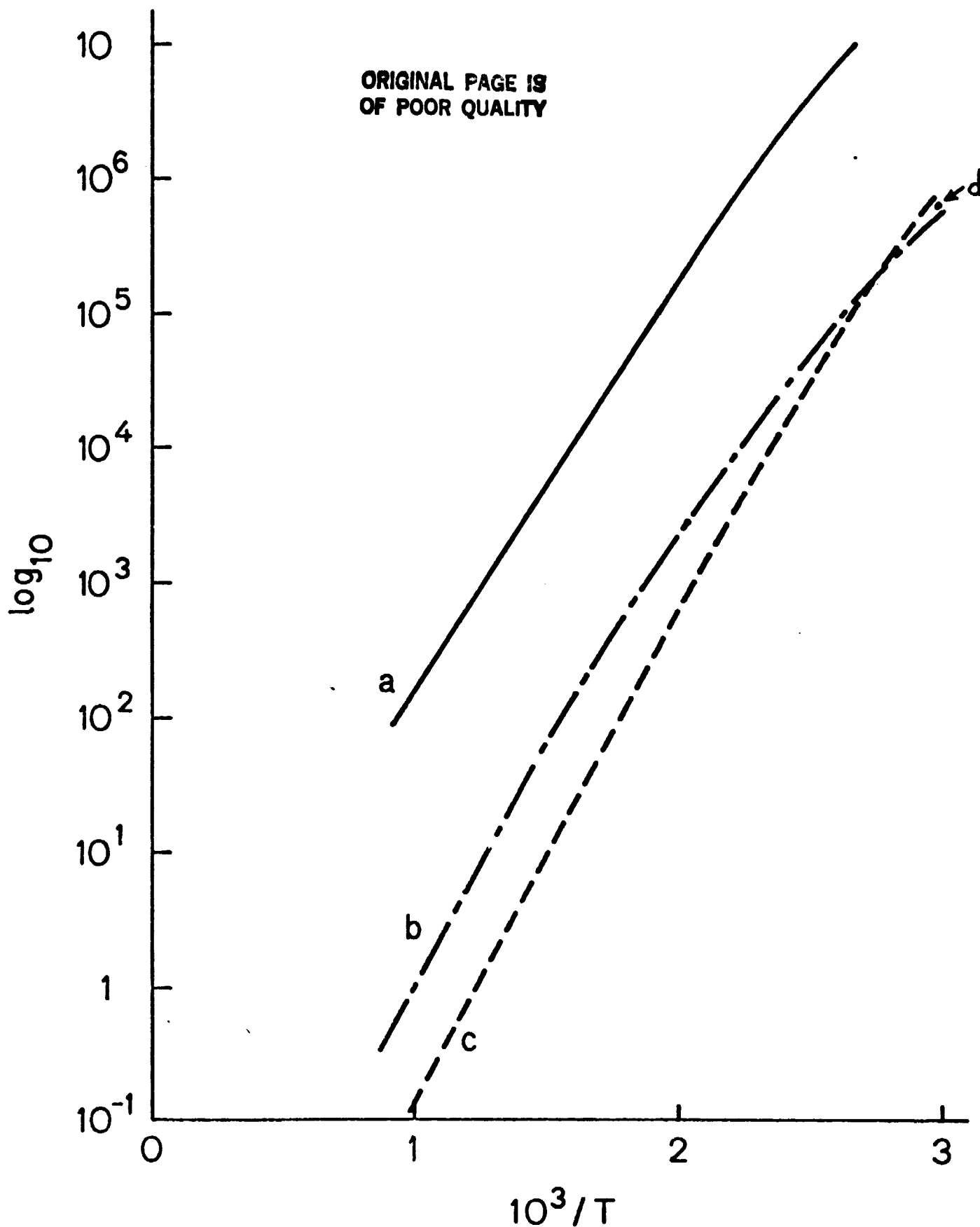


Fig 1. Electrical resistivity of some highly purified  $\beta$ - boron samples. (a) Eubank et al. (3)- vacuum distilled single crystal needles; (b) Eubank et al. (3) hot-pressed; (c) Hagenlocher (4) float-zoned single crystal; (d) Prudenziati (5), 99.9995% pure single crystal.



The mobility of holes in  $\beta$ -boron has been measured by a number of investigators (see Fig 2). Geist and Meyer (6) noticed that the electrical conductivity of illuminated  $\beta$ -B crystals could be correlated with the signal strength of an electron paramagnetic resonance (EPR) line at  $g = 2.0029$ . Adirovich et al. (7) studied the photoconductivity rise time at microwave frequency and also obtained a room temperature hole mobility of the order of  $10^{-4}$  cm<sup>2</sup>/Vs. A similar order of magnitude was indicated by photoconductivity data by Nadolny et al. (8). Also shown in Fig 2 is the range of data from Golikova's review (9). There is clearly a very large scatter between data obtained by different techniques and on different materials, probably because of differences in physical defects and impurity concentrations between the various samples used. There is agreement, however, that the mobility shows an exponential dependence on  $1/T$  with an activation energy in the region of 0.1 eV. It may also be noted that the Hall mobility is generally higher than the drift mobility (9).

The low mobility in boron is probably associated with the presence in the crystal lattice of a high concentration of defects which greatly disturb the three-dimensional order. It has been suggested that boron behaves to a large extent like an amorphous material. This "amorphous concept" has been stressed particularly by Golikova and co-workers (see (9)) although the origin of this behavior has never been clarified. The 8- and 9- coordinated boron atoms, constituting 13% of the total atoms in the lattice, have been associated with the formation of local levels of high charge density. In addition it has been pointed out that because of the complex nature of the lattice and the variation in bond length at different locations, equivalent atoms occur at distances  $\approx 10$  interatomic spacing ( $\approx 17\text{\AA}$ ) so that "hopping" transitions between identical atoms involve very long distances.

The electrical properties of  $\beta$ -boron appear to be mainly determined by the occurrence of traps. The most detailed study of traps is that by Prudenziati (10) who found using a number of different techniques and materials, traps with activation energies of 0.23 or 0.36 eV for holes and 0.25 or 0.44 eV for electrons. What is not clear from this or any other study is the origin of these traps. The concentration of traps is

ORIGINAL PAGE IS  
OF POOR QUALITY

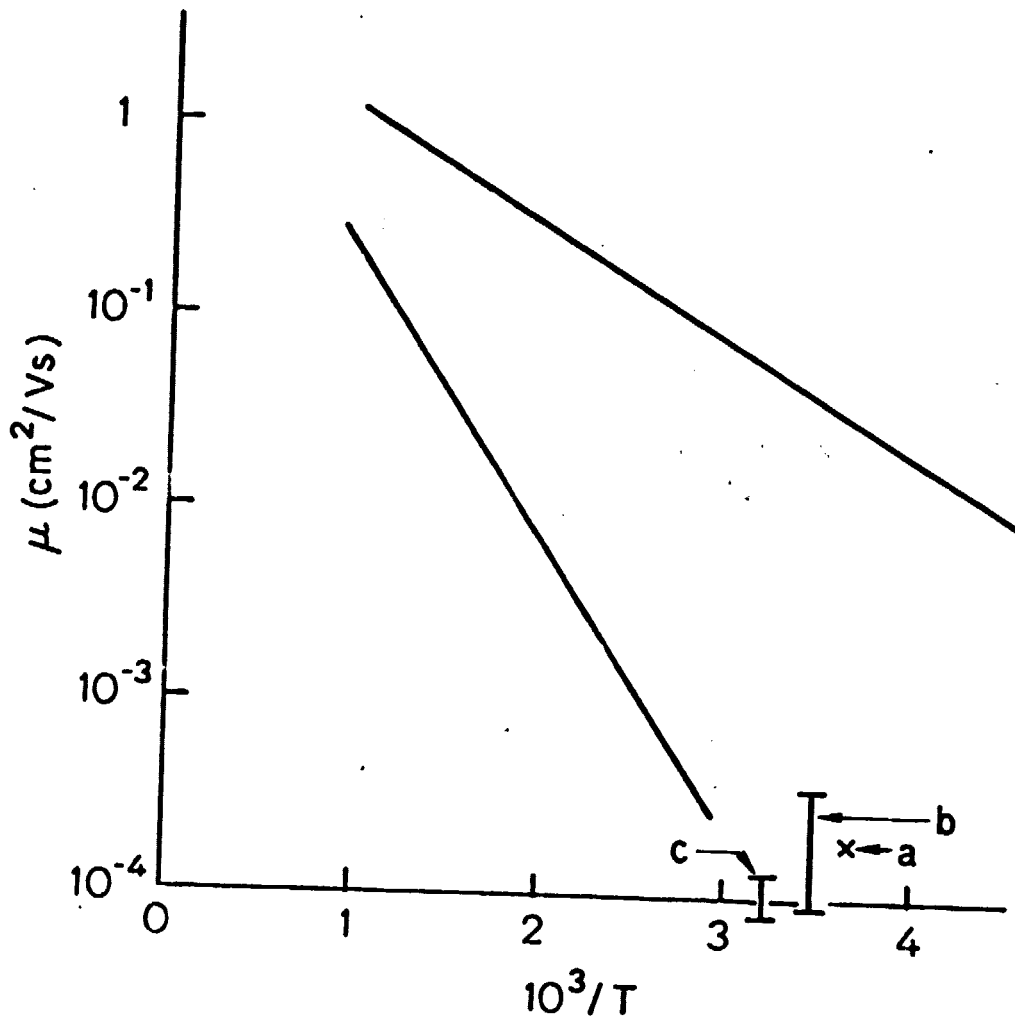


Fig 2. Carrier mobility of positive holes in  $\beta$ - boron (a) Giest and Myer (6) using EPR; (b) A dirovich et al. (7)-Photoconductivity at microwave frequency (c) Nadolny et al. (8)-photoconductivity. The band shows the range of data reported by Colikova (9).

typically found to be  $\approx 10^{20}/\text{cm}^3$  (11), two orders of magnitude higher than the concentration of carbon or other impurities. A high density of imperfections means a disturbance of the lattice periodicity, and hence the occurrence of bound states near the band edges.

Very little is known about physical defects in boron and its solid solutions. Hoard et al. (12), in attempting a detailed structure analysis for  $\beta$ -B, suggested that two sites (labelled 13 and 16) had very low site occupancy factors of 2/3 and 1/3 respectively. Little subsequent data is, however, available on whether the dominant point defects are vacancies or interstitials, and on the condensation of point defects into stacking faults. Twinning was observed by Antadze et al. (13) and by Badzian et al. (14) but was not described in detail. We plan to undertake a more detailed study of defects in  $\beta$ -B, in collaboration with Prof. R. Sinclair who is a leading expert on high resolution electron microscopy.

B. Solid solutions based on the  $\beta$ -boron structure

The practical problems of producing a material of adequate figure-of-merit for the SP100 or similar thermoelectric generators can perhaps be best formulated in terms of an expression for the figure-of-merit due to Chasmer and Stratton (15). They have

$$ZT = (\eta - \delta)^2 [\Delta + 1/\beta\epsilon]^{-1} \quad (1)$$

Here  $\eta = E_F/kT$ ,  $\beta = (K/e)^2 T\sigma_m/K_L$ ,  $\Delta$  and  $\epsilon$  are dimensionless quantities which depend on Fermi integrals and  $\delta$  is the kinetic energy term in the normal expression for the Seebeck coefficient  $\alpha = (k/e) (\eta - \delta)$ . Now  $\eta$ ,  $\Delta$  and  $\epsilon$  will change with the Fermi level and hence with the level of doping in a particular system. The "material parameter"  $\beta$  can be written as

$$\beta = \frac{Ne \mu}{(k/e)^2 K_L} \quad (2)$$

where  $N$  is the density of states,  $\mu$  the carrier mobility and  $K_L$  the lattice contribution to the thermal conductivity. Thus a good material is one with a high density of states, high carrier mobility and low lattice thermal conductivity.

Apart from the choice of doping level, the conceptual problem of material selection therefore reduces to choosing a material with a low defect density (which means increased  $\mu$ ) and one in which the phonon spectrum is disturbed in such a way that  $K_L$  is low. The valence band structure of

ORIGINAL PAGE IS  
OF POOR QUALITY

various borides has been studied using K- and L- xray emission spectra (16).  $B_4C$  and  $B_{13}O_2$  were found to have the lowest bandwidth and relatively complex K-spectra, with  $\alpha$ - and  $\beta$ -B and amorphous boron exhibiting simpler spectra. Ideally it should be possible to make useful predictions about the influence of various alloying elements on  $\mu$  and  $K_L$  based on bonding and crystal chemistry and this is one of the goals of our program although the complexity of the structure and bonding makes it very difficult to achieve in the high-boron materials. As pointed out in our earlier report, it seems to us that a goal of  $ZT=1$  would be difficult to achieve with materials in which the mobility has a substantial activation energy, since a low value of  $\mu$  leads to a very low value of  $ZT$  at the low-temperature end of the thermoelectric junction.

In general, it is found that compounds ranging in composition from  $MB$  to  $MB_6$  (where  $M$  is a cation) are metallic conductors while those based on boron icosahedra are semiconductors. Chemical bonding in boron icosahedra was considered by Longuet-Higgins and Roberts (17). Their molecular orbital calculations suggested that 26 valence electrons fill the bonding molecular orbitals inside the icosahedron, with 12 covalent bonds formed with neighboring atoms. This mean number of bonding electrons would therefore be  $3 \frac{1}{6}$  per boron atom compared with 3 for neutral boron, and the electronic structure will be sensitive to the valence and number of the electrons contributed by the alloying elements.

There is a fairly good accumulated body of data on the location of alloying elements in the  $\beta$ -boron structure, as reviewed by Matkovich and Economy (18). It is clear, for example, that small atoms such as carbon and silicon can replace boron in both interstitial and icosahedral sites, so that true line compounds are likely to be very rare. This is generally confirmed by x-ray data, which shows a range of compositions over which solid solutions with structures based on icosahedral boron exist. As an example, the homogeneity range of boron carbides with the rhombohedral structure was found to extend from  $B_{10.4}C$  to  $B_4C$  (19).

Conductivity and thermoelectric data for various dopants in  $\beta$ -boron are relatively scarce. Good data on materials of high purity, and models of the donor or acceptor properties of various dopants are particularly

conspicuous by their absence. Pracka et al. (10) introduced a number of rare earth and transition metal dopants into  $\beta$ -B and noted that some show a non-uniform distribution even if introduced into the melt. They investigated EPR line intensities, which were expected to be directly related to the carrier concentration, in several samples but observed either a decrease with increasing temperature or a peak at around 500K. The concentration could therefore not be reliably determined from the EPR data. Very recently Rosolowski (21) reported a more useful survey of various dopants in which the change in room temperature resistivity  $\sigma_{RT}$  was determined for concentrations of 1-2 at % of a number of transition metal and other impurities. Co, Cr, Fe and V were found to cause very rapid drops in  $\sigma_{RT}$ , by almost 8 orders of magnitude in the case of vanadium. The resulting materials are n-type, but unfortunately they become p-type at 200-300°C and so the Seebeck coefficient is low since a 2-carrier mechanism is involved.

In an earlier study, Golikova et al. (22) compared the effects of doping with C, Ca and Zr and with combinations of these dopants. 1% Zr + 1% Ca was found to give a particularly high electrical conductivity,  $> 10^2$  (ohm cm)<sup>-1</sup> and 1% Zr alone gave a value above 10 (ohm cm)<sup>-1</sup>. This result contrasts very strongly with that of Rosolowski (21) who found  $\sigma_{RT}=10^{-4}$  (ohm cm)<sup>-1</sup> for 1% Zr doping. The huge discrepancy between the two sets of data illustrate the need for careful sample preparation and characterization. The Soviets unfortunately do not appear to appreciate this problem and do not report sample purity or method of preparation. The promising data reported (22) does suggest, however, a possibility of high conductivities of samples in which Ca-and/or Zr- doping is combined with another element, probably carbon. (Carbon and oxygen are the most common impurities in boron).

In seeking a new criterion which might help identify systems of particular interest, we borrowed from the literature of amorphous materials a parameter Q. This is defined by the equation

$$Q = \frac{c}{k} \alpha + \ln \sigma \quad (3)$$

and is a measure of disorder which has been used, for example, to compare

the effectiveness of hydrogen and other additions in removing dangling bonds in amorphous silicon. For a conventional broad band semiconductor,

$$\sigma = ne\mu \quad \text{with } n = N \left\{ \exp - [E_F(T) - E_V(T)]/kT \right\} \quad (4)$$

so that

$$\ln \sigma = \ln \sigma_m - [E_F(T) - E_V(T)]/kT \quad (5)$$

The Seebeck coefficient is

$$\alpha = \frac{k}{e} \left\{ [E_F(T) - E_V(T)]/kT + \delta \right\} \quad (6)$$

so that, if  $E_F(T) - E_V(T)$  is the same for both conduction and thermoelectricity, then

$$Q = \delta + \ln \sigma_m \quad (7)$$

which is independent of temperature. A plot of  $Q$  versus  $1/T$  is therefore an indication of an activated carrier mobility, which might occur due to disorder or small polaron formation. Representative data is plotted in Fig. 3 for data taken from GA reports or from the literature. (The Si boride data is discussed later). The boron/carbon alloy samples are well behaved according to the criterion proposed. Even a sample with composition  $B_{99}C_{01}$  has a roughly temperature-independent  $Q$ , while samples of higher carbon concentration have substantially higher values of  $Q$  with the same low activation energy. Similarly the Golikova (22)  $B_{99}Zr_{01}$  sample has a high value of  $Q$  with little dependence on temperature. The silicon boride samples, in contrast, have a substantial activation energy, as expected from the separate  $\sigma$  and  $\alpha$  values.

Our general conclusion from this study is that the solution to the choice of a p-type material probably lies in an appropriate ternary composition. The GA boron carbides have good electrical properties (possibly an acceptable  $\alpha^2/\rho$ ) but a high thermal conductivity; in that case the best alloying element would be that which reduces  $K_L$ . The best Soviet samples were probably Zr + (unintentional) C-doped, possibly in combination with Ga. The Si/B samples clearly need a dopant which increases the electrical conductivity.

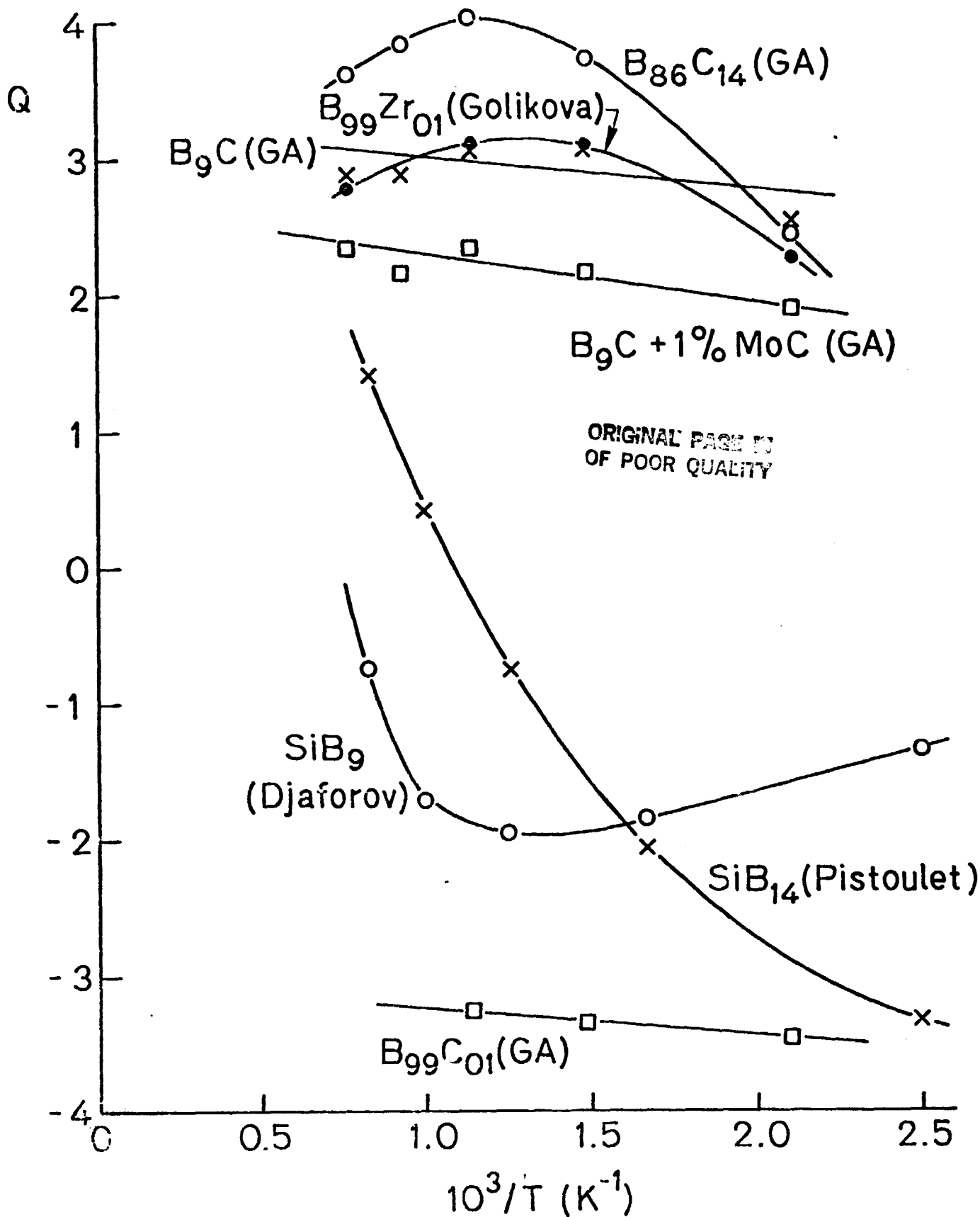


Fig 3. Plots of  $Q = \frac{e\alpha}{K} + \ln \sigma$  versus  $1/T$  for various high-boron materials. Data from GA reports (N. Elsner and co-workers) or from literature quoted in reference list (first-named author listed).

According to our model, the best combination of dopants would not only give a suitable carrier concentration but would also "lubricate" the lattice to increase the mobility by reducing the density of trapping centers. Since so little information is presently available on trapping mechanisms in boron, it is difficult to predict at present what elements would be most effective in this respect.

C. Thermal conductivity

For a given Seebeck coefficient, optimization of the thermoelectric figure-of-merit requires maximization of the electrical conductivity and minimization of the thermal conductivity. Attention is therefore being focused on the basic physical parameters influencing these two conductivities in order to establish logical procedures for performing this optimization. Since charge carriers contribute to both electrical and thermal conductivity, the first requirement for this optimization is maximization of the lattice contribution to thermal conductivity. It has been pointed out by Slack et al. [23] that the dominant contribution to the lattice thermal conductivity is from the acoustic phonons, more than 75% for boron and the boron compounds of particular interest in this program. For this reason, materials with complex unit cells which have a large number of optical phonons, tend to have low lattice thermal conductivity. This is a favorable factor for boron and boron compounds. The magnitude of lattice thermal conductivity is also controlled by the mean free path of the acoustic phonons, as determined by mechanisms of interphonon scattering. A lower limit to this scattering is governed by lattice non-linearity, characterized by the Gruneisen constant  $\gamma$ . Additional increases in phonon scattering - and decreases in thermal conductivity arise from imperfections and any other disorder in the structure. An important example of this phenomenon is found in the behavior of doped SiGe alloys [24]. The basic SiGe alloy has lower thermal conductivity than polycrystals of its two components, because of phonon scattering due to disorder in the alloy. Further enhancement of phonon scattering in these materials is achieved, without strongly affecting the electrical properties, by doping with compatible III-V compounds [23]. Discussions concerning this material are to be held with V. Raag with the aim of better under-



standing the principle involved in enhancing phonon scattering in potential thermoelectric materials. This information will then be applied to our study of boron and boron compounds. A specific goal is the choice of an alloying element to reduce the lattice thermal conductivity of boron carbon compounds without adverse effect on electrical properties.

### III. EXPERIMENTAL

#### A. Silicon borides

Our concentration on silicon borides was mainly undertaken because of very promising results from groups in France and the Soviet Union. Pistoulet and co-workers reported a figure-of-merit  $ZT$  of 1.25 at 1500K and 7 at 2000K (28) for a chemically vapor transported sample of stated composition  $\text{SiB}_{14}$ . Later Dzhafarov et al. (17) reported a room temperature Hall mobility for  $\text{SiB}_9$  of  $15\text{-}70 \text{ cm}^2 \text{ V}^{-1} \text{ s}^{-1}$ , much higher than for any similar material. The initial aims of our experimental program were to clarify the phase diagram, to grow single crystal samples and to confirm or refute the earlier data.

#### 1. Phase diagram

An understanding of the phase diagram of silicon-boron appears essential for the fabrication of reliable samples, especially in view of conflicts in the published data. The earliest diagrams are those of Elliot (28), Knarr (29) and Samsonov (30). Although these differ in the regions of coexistence, they agree on the presence of a line compound  $\text{SiB}_6$ , a phase  $\text{SiB}_3$  or  $\text{SiB}_4$  stable up to  $\sim 1300^\circ\text{C}$  and a solid solution of Si in boron. The limiting solubility is only  $\approx 5 \text{ wt } \%$  according to Samsonov, but  $\approx 15\%$  according to Knarr. Male and Salanoubat (31) measured the liquidus temperature to  $\pm 30^\circ\text{C}$  or so and proposed the existence of a new phase, labelled  $\text{SiB}_n$  with  $n \approx 23$ . Even earlier, Giese et al. (39) claimed another new phase,  $\text{SiB}_{14}$ , on slow cooling a silicon-boron melt. Arabei (39) found that the orthorhombic  $\text{SiB}_6$  phase was of variable composition, and that the  $\text{SiB}_4$  phase extended in stoichiometry down to  $\text{SiB}_{2.8}$ .

Materials likely to be of interest for thermoelectric applications are those from  $\text{SiB}_6$  to the  $\beta$  solid solutions, but we noted that both "promising" thermoelectric compositions  $\text{SiB}_9$  and  $\text{SiB}_{14}$  were in a 2-phase field according to the latest phase diagram (31). Perhaps the most careful

investigation of the complex situation at the high-boron end of the phase diagram was undertaken by Viola and Bouix (34), who found that loosely compacted Si+B powdered mixtures were fully reacted in 1 hour at 1600°C. By measuring the lattice constants and the variation in unit cell size with composition, they found that the maximum solid solubility of Si in  $\beta$ -boron at 1600°C was  $5.6 \pm 0.1$  at %. The composition range from 5.6 at % of Si to 14.3 at % was found to be a 2-phase mixture of  $\beta$ -B solid solution +  $\text{SiB}_6$ . No evidence was found for an " $\text{SiB}_n$ " phase, and the  $\text{SiB}_{14}$  phase of Giese et al. (32) and Pistoulet (26) was found to be the limiting solid solution with an actual composition close to  $\text{SiB}_{17}$ .

Since these observations agreed with our own conclusions from crystal growth experiments, we have recently undertaken a similar study at  $1650 \pm 50^\circ\text{C}$ , extending beyond the limit of 14.3 at % Si of the Viola experiments. It should be mentioned that a very similar study (reaction sintering with measurement of cell parameters) had led Armas et al. (34) to believe in the existence of the  $\text{SiB}_n$  phase with  $\approx 3$  at % Si. Our own study is still incomplete but we present the results of the investigations to date. Samples have been prepared by heating premixed powders of Alfa Si + Alfa crystalline (60 mesh) boron at  $1650 \pm 50^\circ\text{C}$  for 1 hour in an Astro furnace. The composition range covered so far is from 0-22.4 wt % silicon.

Samples with up to 12.5 wt % Si (5.2 at %) show a similar x-ray pattern to  $\beta$ -boron. The most striking difference in the x-ray powder pattern as silicon is added is the progressive disappearance of the (003) and (012) peaks at  $d=8.0$  and  $7.4\text{\AA}$  respectively. These major changes in the diffraction pattern show that significant changes are occurring in the crystal structure on introduction of the silicon atoms. Although the overall structure is maintained, the silicon atoms do not simply substitute for some of the boron but occupy previously unoccupied sites.

Samples with higher concentrations of silicon show  $\text{SiB}_6$  peaks, as expected from the phase diagram, provided that the reaction time is increased to two hours, or if amorphous boron is used in place of the 60-mesh material.

Our observations consistently do not reveal the presence of an " $\text{SiB}_n$ " phase having a structure different from the  $\beta$ -boron solid solution or  $\text{SiB}_6$  (31). We therefore believe that this phase does not exist.

## 2. Crystal Growth (Si+B)

A series of experiments has been performed with the aim of growing single crystals of  $\text{SiB}_6$  and  $\text{SiB}_{17}$  (i.e., the limiting solid solution) large enough for measurements of conductivity and Seebeck coefficient. The earliest experiments used elemental silicon (semiconductor slices or Alfa powder of 3N purity) and powdered crystalline boron (Alfa, 99.7% purity, 60 mesh). They were melted in pyrolytic BN crucibles 1 cm in diameter and with a conical, tapered bottom region, the total charge being  $6 \pm 1$ g. Rapid heating to the liquidus temperature of  $\approx 1900^\circ\text{C}$  was found to result in a severe loss of silicon at this temperature, and so the samples were maintained for  $\approx 12$  hours at  $1450^\circ\text{C}$ , just above the melting point of the silicon, to allow all the silicon to react.

The major problem experienced with these experiments was the tendency of the reactants to separate because of the density difference between boron (or silicon boride) and silicon. The result of slow cooling experiments was therefore a polycrystalline charge of  $\text{SiB}_6$  on top of a layer of solidified silicon. When a higher temperature was used, for a sample of higher boron concentration, the melt tended to migrate out of the crucible, leaving a polycrystalline charge of the limiting solid solution  $\text{SiB}_{17}$ .

In order to prevent the separation of the reactants, Cerac pre-reacted  $\text{SiB}_6$  was used as starting material. This material is of low purity, but could be replaced by pure hot-pressed source material if successful. It was first confirmed that the  $\text{SiB}_6$  could be melted in a small crucible without reacting with the crucible or other major problems.

The  $\text{SiB}_6$  was then mixed with silicon to give a melt of composition 28.6 wt% B + 71.4 wt % Si which appears from the phase diagram to be optimum for crystal growth of  $\text{SiB}_6$  on slowly cooling from  $1850^\circ\text{C}$ . A closely-fitting hot-pressed BN lid was machined and placed on top of the powder charge in order to prevent loss of the silicon by evaporation or migration. This sample was heated at  $1950^\circ\text{C}$  for an hour and then cooled at  $25^\circ\text{C/hr}$ . The experimental arrangement was not really successful, as separation of reactants clearly occurred on melting, and powdered material was left attached to the BN lid, indicating that all the charge had not

ORIGINAL PAGE IS  
OF POOR QUALITY

melted. The re-solidified charge in the bottom of the crucible contained silicon,  $\text{SiB}_6$  and some  $\text{SiB}_{17}$ . Some 7% of the charge was still lost by volatilization.

In a similar experiment with a BN lid, the Cerac  $\text{SiB}_6$  was used in an attempt to grow crystals of the  $\text{SiB}_{17}$  phase. The weight loss in this case was 14.5%, and some small crystals were grown although these were not large enough for electrical measurements. Again the charge did not completely melt, and  $\text{SiB}_6$  crystallites were observed together with the  $\text{SiB}_{17}$  in the re-solidified material.

The BN lid is partially successful, but the failure of the charge to form a homogeneous liquid phase is clearly a major problem. The next series of experiments will utilize larger diameter crucibles (2.5 cm) and submicron-size amorphous boron (Callery) will be used since this has been found to react quite rapidly with the silicon; complete reaction occurs in loosely compacted samples in less than 1 hour at 1650°C.

### 3. Solution Growth

In view of the problems experienced with attempts to grow silicon boride crystals from the elements, the alternative of using a metallic solvent appears attractive. Bouchacourt and Thevenot (35) recently reported the crystallization of  $\text{SiB}_4$  from solutions in Al and Cu. The materials were melted in alumina crucibles at  $\approx 1700^\circ\text{C}$  and cooled at  $200^\circ\text{C/hr}$ . The aluminium yielded  $\text{AlB}_{12}+\text{Si}$ , but the copper yielded  $\text{SiB}_4$  crystals 1-2 mm in size. In principle, larger crystals could be grown by cooling at a slower rate.

In addition, Higashi et al. (36) grew mm size crystals of a number of transition metal borides from aluminum solution on slow cooling from  $1550^\circ\text{C}$ , using  $\approx 1\text{g}$  boron + several g metal in 100g of solution.

Our initial experiments utilized copper, which seems particularly attractive since the phase diagram (37) shows a high solubility for boron; the eutectic at  $1060^\circ\text{C}$  contains 10.7 at % boron. The furnace available for these experiments has a maximum temperature of  $\sim 1500^\circ\text{C}$  but has a Eurotherm controller and programmer so that close temperature control is possible. In the first experiments only 1g boron (Alfa) and 0.4g silicon were mixed with 100g copper but even this small quantity of boron did not dissolve

ORIGINAL PAGE IS  
OF POOR QUALITY

after prolonged heating. The boron was later replaced by the Callery submicron material and it has now been found possible to dissolve 3g in a 100g Cu melt also containing 1.2g Si. Step-wise additions are being used to determine the solubility limit prior to a slow-cooling experiment.

These experiments confirm that many of the problems experienced in our early work are associated with the extremely low reactivity of the Alfa 60 mesh boron. The use of this material will be discontinued in favor of the Callery submicron material. This latter material shows no x-ray peaks and has a very low content of metallic impurities.

#### 4. Hot pressing

The regular program of hot pressing which we had planned in collaboration with Syncal had to be abandoned due to the ThermoElectron takeover, but a small number of experiments was performed at GA Technologies with the kind cooperation of N. Elsner.

Samples of composition  $\text{SiB}_9$  (chosen because of the Dzhafarov (27) data) were hot-pressed at ~8000 psi at 1325°C and 1750°C for 10 minutes. The lower temperature sample was apparently completely reacted even though the starting material was the Alfa 60 mesh boron. The density, however, was very low. The sample fired at 1750°C was of higher density but was still rather porous (see Fig 4). The polished section clearly shows a 2-phase structure, as expected from the phase diagram. The room temperature resistivity is around 2.4 ohm cm and the Seebeck coefficient is 300 $\mu$ V/deg.

The composition of the  $\text{SiB}_{14}$  samples was chosen since this was used by the French group (26). It was pressed at 1800°C, also for 10 minutes at 8000 psi. The porosity was non-uniform, one end of the sample being substantially more porous than the other. Polished sections (Fig 5) show what appear to be traces of a second phase, although this was not detectable in all the regions examined. The resistivity of this sample was =4 ohm cm and the Seebeck coefficient 334  $\mu$ V/deg. The resistivity is low in comparison with the reported range (38) of  $60 - 8 \times 10^4$  ohm cm and the combination of a high Seebeck coefficient and low resistivity is surprising and suggests that this material has great promise. The French material of 60 ohm.cm resistivity had a Seebeck coefficient of only 40  $\mu$ V/deg and so

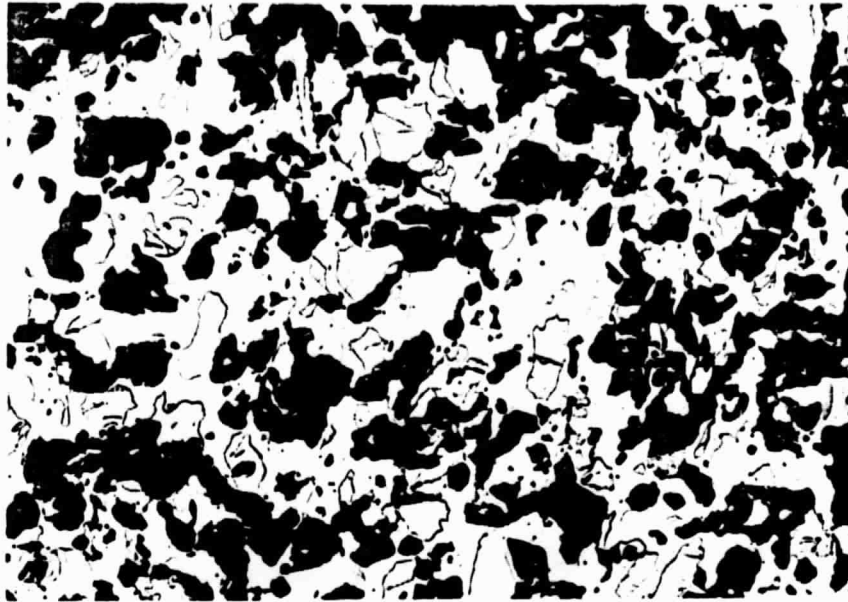


Fig 4. Polished section of hot-pressed  $\text{SiB}_9$ , showing 2-phase structure (250x).

ORIGINAL PAGE IS  
OF POOR QUALITY



Fig 5. Polished section of hot-pressed  $\text{SiB}_{14}$  (620x).

our high value is particularly unexpected. The measurements are, of course, only preliminary but a detailed investigation will be undertaken after the arrival of our hot pressing furnace.

The  $\text{SiB}_9$  and  $\text{SiB}_{14}$  samples were studied in detail by x-ray crystallography in order to obtain an improved understanding of the phase diagram and crystal structure. Table 1 gives a summary of the d spacing and intensities for  $\text{SiB}_{14}$  and  $\text{SiB}_9$  in comparison with  $\beta$ -boron. The  $I/I_0$  values quoted for this material (Alfa) are our experimental values but the pattern is in very good agreement with the ASTM data (39). The  $\text{SiB}_{14}$  data is very similar to that of  $\beta$ -B except for major changes in intensity of several peaks. Only one significant peak, at  $d = 1.855\text{\AA}$ , could not be detected in the  $\beta$ -boron pattern. The two peaks at  $d = 8.0$  and  $7.4\text{\AA}$  could not be seen in the  $\text{SiB}_{14}$  pattern and appear to be the best way of distinguishing boron from its solid solution using this method.

$\text{SiB}_9$  has a similar x-ray pattern to  $\text{SiB}_{14}$ , again with substantial changes in intensity. Since  $\text{SiB}_6$  was expected to be present from the phase diagram and from metallographic examination, the presence of this phase was expected to be confirmed by the x-ray pattern. The major peak of  $\text{SiB}_6$  is at  $4.92\text{\AA}$  (40) and a new peak induced at  $4.95\text{\AA}$  does indeed appear in the  $\text{SiB}_9$  pattern. The  $d = 4.20\text{\AA}$  peak provides additional confirmation of the presence of  $\text{SiB}_6$ .

It can therefore be concluded that the Soviet material (27) for which a high mobility was reported was certainly 2-phase, as suggested by the various phase diagrams, unless the quoted composition of  $\text{SiB}_9$  is very inaccurate.

#### B. Boron suboxide

In our previous report, we referred to unsuccessful attempts to prepare boron suboxide  $\text{B}_6\text{O}$  (also quoted as  $\text{B}_7\text{O}$  or  $\text{B}_{13}\text{O}_2$ ). This material has the advantages of fairly low thermal conductivity, stability up to  $\sim 1800^\circ\text{C}$ , and has a valence band structure similar to that of boron carbides (41). There appear, however, to be no measurements in the literature of electrical conductivity and Seebeck coefficient.

During the visit to GA Technologies, one sample of Alfa crystalline boron (60 mesh) +  $\text{B}_2\text{O}_3$  with 1% Si doping was hot pressed in a BN-lined

ORIGINAL PAGE IS  
OF POOR QUALITYTable 1 Xray Diffraction Data For Hot-Pressed Samples

<u><math>\beta</math>-Boron</u>			<u>SiB<sub>14</sub></u>		<u>SiB<sub>9</sub></u>	
<u>d</u>	I/I <sub>0</sub>	hkl	<u>d</u>	I/I <sub>0</sub>	<u>d</u>	I/I <sub>0</sub>
8.0	30	003				
7.4	25	012				
5.48	20	110	5.50	45	5.50	30
5.06	100	104	5.06	100	5.10	100
					4.95	45
4.65	70	021	4.70	60	4.75	55
4.50	35	113	4.45	35		
4.40	25	202				
4.25	30	015	4.28	55	4.30	45
					4.20	10
3.97	20	006	3.97	70	4.00	90
3.71	25	024	3.75	20	3.75	10
3.54	25	211	3.60	20		
3.43	15	122				
3.07	10	214				
2.94	10	303	2.93	15	2.90	40
2.865	30	125	2.89	45	2.85	40
2.76	5	027	2.77	40	2.79	60
2.73	10	220			2.69	20
2.65	10	009				
2.61	10	131	2.60	35		
2.56	20	312				
2.52	15	208				
2.47	35	217, 306	2.49	45	2.50	60
2.40	15	134	2.43	40	2.44	45
2.32	10	042				
2.24	8	226				
2.13	5	322				
2.04	10	235				



Table 1 Xray Diffraction Data For Hot-Pressed Samples

<u><math>\beta</math>-Boron</u>			<u>SiB<sub>14</sub></u>		<u>SiB<sub>9</sub></u>	
<u>d</u>	<u>I/I<sub>0</sub></u>	<u>hkl</u>	<u>d</u>	<u>I/I<sub>0</sub></u>	<u>d</u>	<u>I/I<sub>0</sub></u>
1.818	5		1.855	15	1.852	15
1.755	15	055	1.775	15	1.815	15
					1.74	55
					1.71	25
1.675	5	425				
1.60	20	515				
1.548	10	432	1.57	35	1.572	25
			1.51	20	1.51	15
1.465	5	066	1.485	15	1.485	15
1.430	12	437	1.425	15	1.445	15
1.402	5	614	1.405	55	1.404	40
1.380	10	438	1.370	70	1.374	60
1.345	10	443	1.357	50	1.36	10
1.307	5	535				
1.237	5	538	1.245	75	1.245	80

ORIGINAL DOCUMENT  
OF POOR QUALITY

graphite die at 1800°C. This die unfortunately failed after about 1 minute at this temperature, but the x-ray diffraction pattern showed strong  $B_6O$  peaks with small  $SiB_6$  peaks. Previous studies had suggested that Si and other elements can catalyze the  $B + B_2O_3$  reaction, but the evidence from this one sample suggests that the Si does not have a significant role, since it forms a second phase rather than being incorporated into the  $B_6O$  lattice. Unfortunately there was not time at GA to press the other sample, which was undoped.

The encouraging feature of the  $B_6O$  sample is that the x-rays did not reveal any  $B_2O_3$ , which was found to be present as a major impurity in materials which we had obtained from the earlier Wright Patterson work (42), see Fig 6a. Only lines of  $B_6O + SiB_6$  could be detected in our hot pressed sample even though the firing time was only 1 minute. The major disadvantage of the sample was that the porosity was very high (Fig 6b). The resistivity at room temperature of this sample was  $\approx 10^4$  ohm cm.

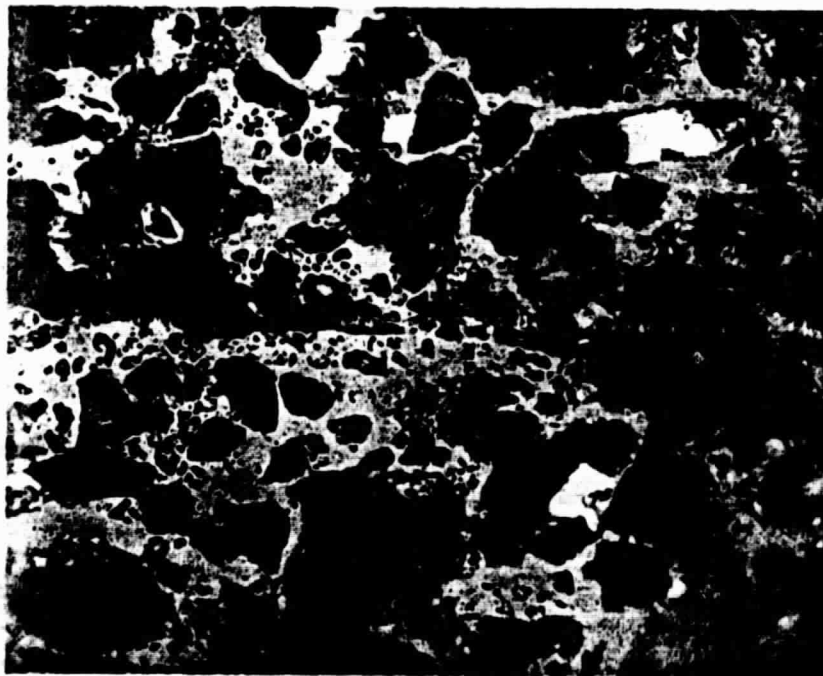
Our previous failure to form  $B_6O$  by cold pressing and sintering was attributed to the low reactivity of the Alfa 60 mesh crystalline boron. A comparative study was therefore undertaken in which boron was mixed with  $B_2O_3$ , die-pressed at room temperature and heated to 1650°C for four hours. One sample used the Alfa 60 mesh boron, the other used Callery amorphous boron. As predicted, the sample made from Alfa boron did not show any trace of  $B_6O$  in its x-ray pattern. However the sample made from Callery boron showed  $B_6O$  as its major constituent. The sample was not completely reacted, and showed  $B_2O_3$  lines as well as a broad region, possibly indicating the presence of unreacted amorphous boron. Although the sample did not densify well, and hot-pressing is clearly preferable to sintering as a means of fabricating samples, this study did confirm the low reactivity of the Alfa boron. The observation that, in spite of this low reactivity, hot-pressing gave a fully reacted sample in only one minute at 1800°C is strong evidence of the value of this fabrication technique.

### C. Thermal capacity of boron carbides.

As a contribution to the GA investigation of boron carbides as high temperature thermoelectric materials, the thermal capacity of three boron-carbide samples was measured using a DuPont Differential Scanning



(a)



(b)

Fig 6. (a) Optical micrograph of hot-pressed  $B_6O$  from the work of Rizzo et al. (42), showing  $B_2O_3$  inclusions; (b) Very porous Hot-pressed  $B_6O$  with  $SiB_6$  as second phase

Calorimeter. Unfortunately this instrument is currently limited to a maximum temperature of 600°C, so extrapolation to the useful range is necessary. The thermal capacity is required in order to convert thermal diffusivity data into thermal conductivity.

Our measurements are shown in Fig. 7 for all three samples. The value of  $C_p$  levels off in each above  $\approx 300^\circ\text{C}$  so major changes above 600°C are not likely. In each case  $C_p \approx 1.5 \text{ J/g/deg}$  and the differences between the three samples are probably not significant.

#### D. Fiber crystal growth

Renewed attempts were made to grow single crystal fibers of  $\text{B}_3\text{C}$  using GA hot-pressed material as the source. This source material must be ground to a cross section less than  $0.5 \times 0.5 \text{ mm}$  section with a length of over 1 cm. There is now enough power in the laser to melt the tip of the  $\text{B}_3\text{C}$  source rod, but the heating is very non-uniform and so a stationary sample was observed to volatilize in the region heated most strongly while other parts of the tip remained solid. Rotation of the sample is desirable in order to even out the heating but it has been found difficult to grind this very hard material with sufficient precision to prevent lateral excursions of the tip (and consequent temperature fluctuations) during rotation.

Techniques have recently been developed for centerless grinding of brittle materials and attempts will be made to produce 0.5 mm diameter rods of  $\text{B}_3\text{C}$  and silicon borides.

#### IV. SUMMARY OF MAIN CONCLUSIONS

1. The most important adverse factor towards the development of high boride materials of high figure-of-merit appears to be trapping of the charge carriers, which results in a low mobility. The nature of the traps has never been determined.
2. No evidence was found to support the existence of an " $\text{SiB}_n$ " phase having a structure different from  $\text{SiB}_6$  or the limiting solid solution. The x-ray powder pattern of the limiting solid solution  $\text{SiB}_{17}$  shows significant differences from  $\beta$ -boron, but can be indexed on the same basis.
3. Attempts to grow single crystals of  $\text{SiB}_6$  and  $\text{SiB}_{17}$  from Si-B melts were not successful, mainly because of Si volatilization and the problems of producing a homogeneous melt. The low reactivity of crystalline boron was

ORIGINAL PAPER IS  
OF POOR QUALITY

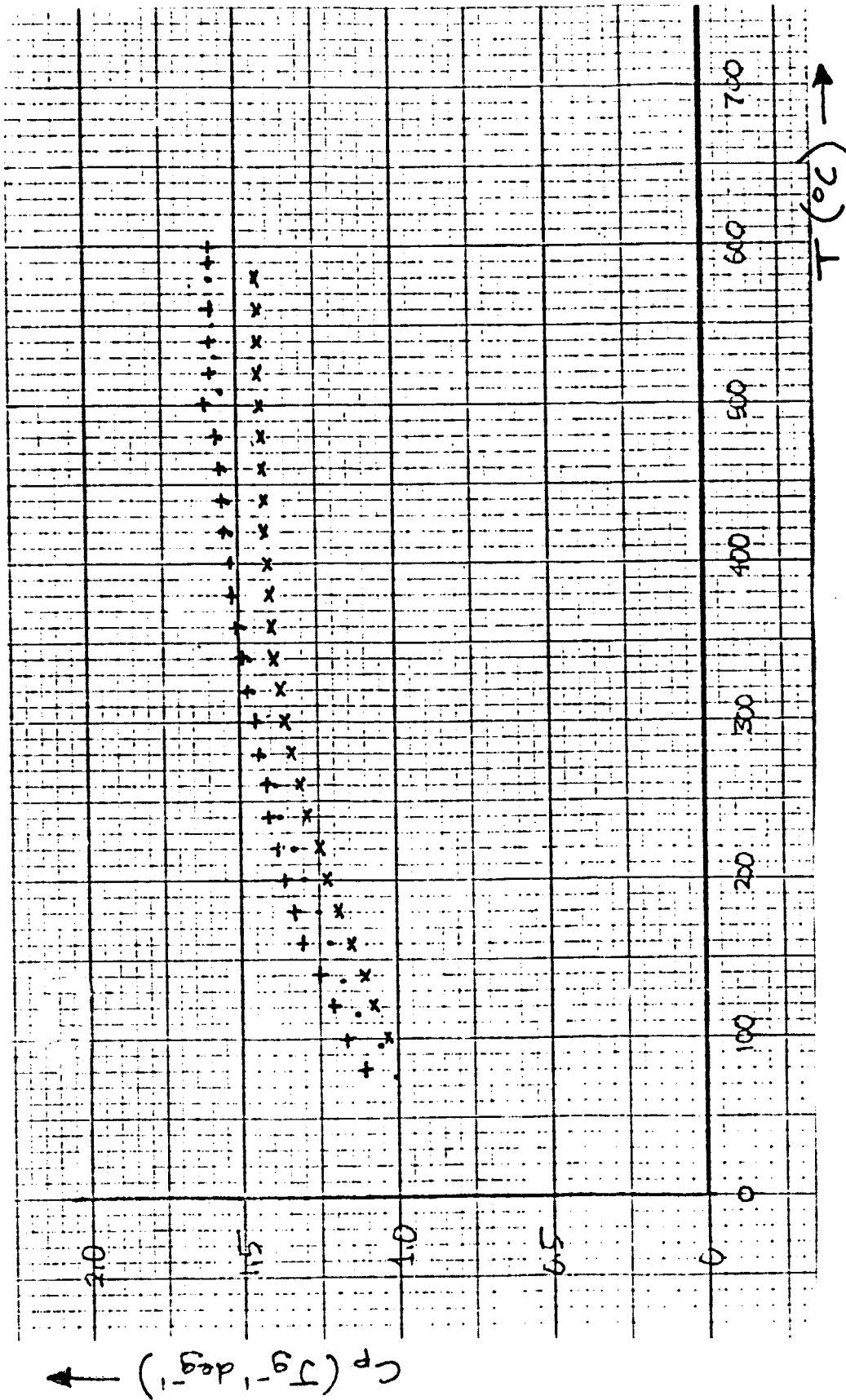


Fig 7. Heat capacity  $C_p$  of boron carbides:  
 $B_{13}C_2$ ; x  $B_9C$ ; +  $B_9C$

also a problem in growing crystals from copper solutions, but the introduction of amorphous boron has greatly facilitated materials synthesis.

4. Samples of  $\text{SiB}_9$  and  $\text{SiB}_{14}$  were hot-pressed at GA. The  $\text{SiB}_9$  clearly exhibits a 2-phase structure, and throws doubts on Soviet reports on this material. However the room temperature electrical conductivity and Seebeck coefficient of these materials look promising.

5. Boron suboxide  $\text{B}_6\text{O}$  was successfully synthesized by hot-pressing. The feasibility of synthesis by cold-pressing and sintering of amorphous boron +  $\text{B}_2\text{O}_3$  was also demonstrated, in contrast to a sample of crystalline boron +  $\text{B}_2\text{O}_3$  which showed no reaction.

6. The material which is eventually selected as the p-leg of the thermocouple for SP-100 will probably be a ternary composition eg  $\text{B}_{1-x-y}\text{C}_x\text{Si}_y$ .

The evidence suggests that such materials, based on boron icosahedra, are all solid solutions rather than line compounds.

#### V. WORK PLAN - next 6 months

A major advance in the rate of acquisition of data is expected within the next month following the arrival of an Astro Hot Pressing Furnace and the construction of apparatus for measurement of electrical conductivity and Seebeck coefficient. The hot press will be used for pre-reaction of samples for crystal growth experiments and for the fabrication of samples for measurement of electrical properties. Initially this part of the program will be concentrated on silicon borides and on a study of dopants which lead to a higher mobility for positive holes in  $\beta$ -boron and related materials.

It is also hoped to identify the physical defects responsible for carrier trapping in  $\beta$ -boron using high resolution electron microscopy. Vapor-grown crystals for this study have been kindly provided by Kelly Meares of Eagle-Picher. The problem of reducing the incidence of traps appears to us to be the key area in producing boride materials of high figure of merit.

Theoretical studies will also be aimed at tailoring materials of lower thermal conductivity.

Experiments aimed at clarifying the Si-B phase diagram will be concluded and should be of great value for sample fabrication. Crystal growth experiments will continue and will include slow cooling in larger diameter crucibles and closed-space vapor transport. Solution growth experiments using copper will continue, and Al or Sn will be tried as alternative solvents for silicon borides. Fiber crystal growth will be re-attempted using ground source rods.

Since accumulating evidence suggests that it will be difficult to make a high temperature n-type boride, we plan to begin some work on a rare earth chalcogenide, probably  $\text{La}_4\text{Te}_7$ .

ORIGINAL PAGE IS  
OF POOR QUALITY

VI. REFERENCES

1. R. E. Hughes, C. H. L. Kennard, D. B. Sullenger, H. A. Weaklein, D. E. Sands, and J. L. Hoard, J. Am. Chem. Soc. 85 (1963) 361.
2. R. A. Brungs in "Boron," Vol. 2 (Ed. G. K. Gaulé) Plenum, New York, 1965, p. 119.
3. W. R. Ewbank, L. E. Pruitt, and H. Thurnauer in "Boron," (Ed. J. A. Kohn, W. F. Nye and G. K. Gaulé) Plenum, New York, 1960, p. 116.
4. A. K. Hagenlocher in "Boron," (Ed. J. A. Kohn, W. F. Nye and G. K. Gaulé) Plenum, New York, 1960, p. 128.
5. M. Prudenziati, Phys. Stat. Sol. (1) 3 (1970) K81.
6. D. Geist and J. Meyer, Proc. 10th Intl. Conf. Semiconductor Physics, 1970, p. 597.
7. E. I. Adirovich, V. A. Benderskii, V. K. Brikshtein, and Y. A. Korostelev, Soviet Phys. Semicond. 5 (1971) 8.
8. A. J. Nadolny, A. Zareba, M. Igalson, and N. T. Dung, J. Less-Comm. Met. 47 (1976) 119.
9. O. A. Colikova, Phys. Stat. Sol. (a) 51 (1979) 11.
10. M. Prudenziati, J. Less-Comm. Met. 47 (1976) 113.
11. H. Werheit, Phys. Stat. Sol. 39 (1970) 109.
12. J. L. Hoard, D. B. Sullenger, C. H. L. Kennard, and R. E. Hughes, J. Solid State Chem. 1 (1970) 268.
13. M. E. Antadze, D. A. Avlokhavili, A. G. Khuedelidze, G. F. Tavadze, G. V. Tsagareshvili, and F. N. Tavadze, J. Less Comm. Met. 47 (1976) 243.
14. A. R. Badzion, A. Klokocki, and T. Niemyski in "Boron," Vol. 3 (Ed. T. Niemyski), PWN Warsaw, 1970, p. 147.
15. R. P. Chasmar and R. Stratton, J. Electronics & Control 7 (1959) 52.
16. E. P. Domashevskaya, N. E. Solovjev, V. A. Terekhov, and Y. A. Ygal, J. Less Comm. Met. 47 (1976) 189.
17. H. C. Longuet-Higgins and M. de V. Roberts, Proc. Roy. Soc. A230 (1955) 110.



18. V. I. Matkovich and J. Economy in "Boron and Refractory Borides," (Ed. V. I. Matkovich) Springer Verlag, 1977, p. 96.
19. M. Bouchacourt and F. Thevenot, *J. Less-Comm. Met.* 82 (1981) 219.
20. I. Pracka, J. Jun, T. Niemyski, and R. Jablonski in "Boron," Vol. 3 (Ed. T. Niemyski), Polish Scientific Publishers, 1970, p. 57.
21. J. Rosolowsky, Proc. 1982 Working Group on Thermoelectrics, NASA/JPL, p. 441.
22. O. A. Golikova, V. K. Zaitsev, A. V. Retrov, L. S. Stilbans, and E. N. Tkalenko, *Sov. Phys. Semicond.* 6 (1972) 1488.
23. G. A. Slack, D. W. Oliver and F. H. Horn, *Phys. Rev.* B4 (1971) 1714.
24. J. P. Dismukes, L. Ekstrom, E. F. Steigmeier, I. Kudman, and D. S. Beers, *J. Appl. Phys.* 35 (1964) 2899.
25. V. Raag, Private Communication.
26. R. Pistoulet, J. L. Robert, J. M. Dusseau, F. M. Roche, and P. Girard, Proc. 1978 Int. Conf. Phys. Semicond., Inst. Phys. (UK) #43, p. 793.
27. E. A. Dzhafarov, O. A. Golikova and M. I. Aliev, *Dokl. Akad. Nauk. Az SSR* 36 (1980) 23.
28. R. P. Elliot, *Constitution of Binary Alloys*, 1st Suppl., McGraw Hill, New York, 1965.
29. W. A. Knarr, Thesis, Univ. of Kansas, 1969.
30. G. V. Samsonov and V. M. Spletsov, *Dopovidi Akad. Nauk. Ukr. RSR* 8 (1962) 1066; see 28.
31. G. Malé and D. Salanoubat, *Rev. Int. Haut. Temp. Refract. Fr.* 18 (1981) 109.
32. R. F. Giese, J. Economy and V. I. Matkovich, *Z. Krist.* 122 (1965) 144.
33. B. G. Arabei, *Inorg. Mat. USSR* 15 (1979) 1251.
34. B. Armas, G. Malé, D. Salanoubat, C. Chatillon, and M. Allibert, *J. Less-Comm. Met.* 82 (1981) 245.
35. M. Bouchacourt and F. Thevenot, *Mat. Res. Bull.* 17 (1982) 1353.
36. I. Higashi, Y. Takahashi and T. Atoda, *J. Crystal Growth* 33 (1976) 207.
37. F. Lihl and O. Fleischl, *Metall.* 8 (1954) 11.

38. B. Armas, C. Combescure, J. M. Dusseau, T. P. Lepetre, J. L. Robert, and R. Pistoulet, J. Less-Comm. Met. 47 (1976) 135.
39. Sands and Hoard, J. Am. Chem. Soc. 79 (1957) 5582.
40. ASTM card 14-92, material from C. J. Cline, J. Electrochem. Soc. 106 (1959) 342.
41. E. P. Domashevskaya, N. E. Solovjev, V. A. Terekhov, and Y. A. Ugai, J. Less-Comm. Met. 47 (1976) 189.
42. H. F. Rizzo, W. C. Simmons, and H. O. Bielstein, J. Electrochem. Soc. 109 (1962) 1079.